

**UniMAP**

**Structure and Properties of Cathode and  
Electrolyte for Intermediate Temperature Solid  
Oxide Fuel Cells (IT-SOFCs)**

**By**

**Nurhamidah Binti Zakaria  
(1430411328)**

A thesis submitted in fulfillment of the requirements for the degree of  
Master of Science in Materials Engineering

**School of Materials Engineering  
UNIVERSITI MALAYSIA PERLIS**

2017

## UNIVERSITI MALAYSIA PERLIS

### DECLARATION OF THE SIS

Author's full name : NURHAMIDAH BINTI ZAKARIA  
Date of birth : 1<sup>st</sup> MARCH 1990  
Title : STRUCTURE AND PROPERTIES OF CATHODE AND  
ELECTROLYTE FOR INTERMEDIATE TEMPERATURE SOLID  
OXIDE FUEL CELLS  
Academic Session : 2016/2017

I hereby declare that the thesis becomes the property of Universiti Malaysia Perlis (Unimap) and to be placed at the library of Unimap. This thesis is classified as :

- CONFIDENTIAL** (Contains confidential information under the Official Secret Act 1972)\*
- RESTRICTED** (Contains restricted information as specified by the organization where research was done)\*
- OPEN ACCESS** I agree that my thesis is to be made immediately available as hard copy or on-line open access (full text)

I, the author, give permission to the Unimap to reproduce this thesis in whole or in part for the purpose of research or academic exchange only (except during a period of \_\_\_\_\_ years, if so requested above).

Certified by:

\_\_\_\_\_  
SIGNATURE  
900301065558  
(NEWIC NO / PASSPORT NO.)

Date : \_\_\_\_\_

\_\_\_\_\_  
SIGNATURE OF SUPERVISOR  
DR. MOHD SOBRI IDRIS  
NAME OF SUPERVISOR

Date : \_\_\_\_\_

NOTE 8 : \* If the thesis is CONFIDENTIAL or RESTRICTED, please attach with the letter from the organization with period and reasons for confidentiality or restriction.

## ACKNOWLEDGEMENT

In the name of Allah S.W.T. The Most Gracious and Merciful.

Alhamdulillah and thanks to Allah because of His Bless, finally I succeed to complete the given task in a proper and organize manner. First of all, thank my supervisor, Dr Mohd Sobri Idris, he teaches me how to work independently. His guidance, encouragement, and enthusiasm for research has truly helped me make it this far.

Also, thanks to my ex-supervisor, En Murizam Darus for his support to complete this thesis. A lot of thanks to Dr Rozana Aina Maulat Osman for her continue assistance, uncountable help and guidance, throughout the whole process to complete my research.

My gratitude is also extended to lecturers and technicians of School of Materials Engineering, UNIMAP, for assisting in putting my research work into action and for their help and guidance during laboratory works. Many thanks also to my Electronics Materials Group and my fellow friends.

Finally, I would also give my special appreciation to my adore family members for their unconditional love and support my entire life and brought me up to this level. Last but not least, thank you to all the people around me who involved in this research neither directly nor indirectly.

## TABLE OF CONTENTS

	<b>PAGE</b>
<b>THESIS DECLARATIONS</b>	i
<b>ACKNOWLEDGEMENT</b>	ii
<b>TABLE OF CONTENT</b>	iii
<b>LIST OF TABLES</b>	vii
<b>LIST OF FIGURES</b>	viii
<b>LIST OF ABBREVIATIONS</b>	xii
<b>LIST OF SYMBOLS</b>	xiv
<b>LIST OF EQUATIONS</b>	xv
<b>ABSTRAK</b>	xvi
<b>ABSTRACT</b>	xvii
<b>CHAPTER 1 INTRODUCTION</b>	
1.1 Solid Oxide Fuel Cells (SOFCs)	1
1.2 Properties of SOFCs components	4
1.2.1 Electrolytes	4
1.2.2 Anode	5
1.2.3 Cathode	5
1.3 Problem Statement	6
1.4 Objectives	7
1.5 Scope of Study	8
<b>CHAPTER 2 LITERATURE REVIEW</b>	
2.1 Cathode Materials for IT-SOFCs	9

2.1.1	Phase analysis of $\text{Ba}_{0.5}\text{Sr}_{0.5}\text{Co}_{0.8}\text{Fe}_{0.2}\text{O}_{3-\delta}$	12
2.1.2	Crystal structure of $\text{Ba}_{0.5}\text{Sr}_{0.5}\text{Co}_{0.8}\text{Fe}_{0.2}\text{O}_{3-\delta}$	17
2.2	Electrolyte Materials for IT-SOFCs	20
2.2.1	Overview of ceria based materials	22
2.2.2	Phase analysis of $\text{Ce}_{0.8}\text{Sm}_{0.2}\text{O}_{1.9}$	24
2.2.3	Crystal structure of $\text{Ce}_{0.8}\text{Sm}_{0.2}\text{O}_{1.9}$	26
2.2.4	Ionic conductivity of $\text{Ce}_{0.8}\text{Sm}_{0.2}\text{O}_{1.9}$	27
2.3	The Half Cells of Cathode and Electrolyte Performance of IT-SOFCs	31

### CHAPTER 3 RESEARCH METHODOLOGY

3.1	Material Synthesis	35
3.1.1	Preparation of cathode	35
3.1.2	Preparation of electrolyte	38
3.1.3	Preparation of half cells	40
3.2	Materials Characterisation	42
3.2.1	Structural analysis	42
3.2.2	Electrical and electrochemical analysis	47
3.2.3	Microstructural analysis	50

### CHAPTER 4 RESULTS AND DISCUSSION

4.1	Introduction	51
4.2	Characterisation of Cathode	52
4.2.1	XRD analysis of $\text{Ba}_{0.5}\text{Sr}_{0.5}\text{Co}_{0.8}\text{Fe}_{0.2}\text{O}_{3-\delta}$	52
4.2.2	XRD analysis of an analogous of $\text{Ba}_{0.5}\text{Sr}_{0.5}\text{Co}_{0.8-y}\text{Fe}_{0.2+y}\text{O}_{3-\delta}$ ( $0.2 \leq y \leq 0.8$ )	57
4.2.3	Microstructure analysis of $\text{Ba}_{0.5}\text{Sr}_{0.5}\text{Co}_{0.8}\text{Fe}_{0.2}\text{O}_{3-\delta}$	62

4.2.4	Structural analysis of Rietveld Refinement: Introduction of initial model	63
4.2.5	The structural analysis of $\text{Ba}_{0.5}\text{Sr}_{0.5}\text{Co}_{0.8}\text{Fe}_{0.2}\text{O}_{3-\delta}$	64
4.2.6	The structural analysis of $\text{Ba}_{0.5}\text{Sr}_{0.5}\text{Co}_{0.8-y}\text{Fe}_{0.2+y}\text{O}_{3-\delta}$ ( $0.2 \leq y \leq 0.8$ )	67
4.3	Characterisation of electrolyte	71
4.3.1	XRD analysis of $\text{CeO}_2$	71
4.3.2	XRD analysis of $\text{Ce}_{0.8}\text{Sm}_{0.2}\text{O}_{1.9}$ (prepared)	72
4.3.3	Structural Analysis of $\text{CeO}_2$ and $\text{Ce}_{0.8}\text{Sm}_{0.2}\text{O}_{1.9}$ (prepared and commercial)	78
4.3.4	Microstructure Analysis of $\text{Ce}_{0.8}\text{Sm}_{0.2}\text{O}_{1.9}$ (prepared and commercial)	82
4.3.5	Electrical properties of $\text{CeO}_2$	83
4.3.6	Electrical properties of $\text{Ce}_{0.8}\text{Sm}_{0.2}\text{O}_{1.9}$ (prepared)	88
4.3.7	Comparative study of electrical properties of prepared and commercial $\text{Ce}_{0.8}\text{Sm}_{0.2}\text{O}_{1.9}$	93
4.4	Electrochemical performance of BSCF SDC BSCF half cells	96
4.4.1	The half-cell performances of $\text{Ba}_{0.5}\text{Sr}_{0.5}\text{Co}_{0.8}\text{Fe}_{0.2}\text{O}_{3-\delta}$	96
4.4.2	The analogous of half-cell performance of BSCF SDC BSCF	99
<b>CHAPTER 5 CONCLUSION AND RECOMMENDATIONS</b>		
5.1	Conclusion	102
5.2	Recommendations for Future Works	103
5.3	Commercialization Potential	104
<b>REFERENCES</b>		
105		
<b>APPENDICES</b>		
111		
<b>LIST OF PUBLICATIONS</b>		
114		

## LIST OF TABLES

NO		PAGE
2.1	Structural properties of $\text{Ba}_{0.5}\text{Sr}_{0.5}\text{Co}_{0.8}\text{Fe}_{0.2}\text{O}_{3-\delta}$ (ICDS No: 109462) (Koster & Mertins, 2003).	19
2.2	Refined crystallography parameter in Rietveld analysis of $\text{Ce}_{0.8}\text{Sm}_{0.2}\text{O}_{1.9}$ (Yashima & Takizawa, 2010)	27
2.3	A summary of ASR values of $\text{Ba}_{0.5}\text{Sr}_{0.5}\text{Co}_{0.8}\text{Fe}_{0.2}\text{O}_{3-\delta}$ by various firing temperature.	34
3.1	Capacitance values and their possible interpretation (Irvine et al., 1990)	49
4.1	Crystallite size of $\text{Ba}_{0.5}\text{Sr}_{0.5}\text{Co}_{0.2+y}\text{Fe}_{0.8-y}\text{O}_{3-\delta}$ ( $0 \leq y \leq 0.8$ ) at $900^\circ\text{C}$ for 15 hours as a function cobalt concentration.	61
4.2	The initial structural model $\text{Ba}_{0.5}\text{Sr}_{0.5}\text{Co}_{0.8}\text{Fe}_{0.2}\text{O}_{3-\delta}$ (ICDS No:109462)	63
4.3	Refined structural data using the obtained $U_{\text{iso}}$ values for the $\text{Ba}_{0.5}\text{Sr}_{0.5}\text{Co}_{0.8}\text{Fe}_{0.2}\text{O}_{3-\delta}$ synthesised from $900$ to $1100^\circ\text{C}$ in air.	64
4.4	Refined structural data using the obtained $U_{\text{iso}}$ values for the $\text{Ba}_{0.5}\text{Sr}_{0.5}\text{Co}_{0.8-y}\text{Fe}_{0.2+y}\text{O}_{3-\delta}$ ( $0.0 \leq y \leq 0.8$ ) synthesised at $900^\circ\text{C}$ for 15 hours in air.	68
4.5	Summary of lattice parameter, unit cell volumes and crystallite size of pure phase of $\text{Ce}_{0.8}\text{Sm}_{0.2}\text{O}_{1.9}$ (prepared) $\text{Ce}_{0.8}\text{Sm}_{0.2}\text{O}_{1.9}$ (commercial) and $\text{CeO}_2$ .	77
4.6	Starting model of structural refinement of $\text{CeO}_2$ ICSD No: 28753	78
4.7	The initial structure model for $\text{Ce}_{0.8}\text{Sm}_{0.2}\text{O}_{3-\delta}$ ICSD No: 182979	79
4.8	Structural data of $\text{CeO}_2$ and $\text{Ce}_{0.2}\text{Sm}_{0.8}\text{O}_{3-\delta}$ (commercial and prepared) powder obtained from Rietveld refinement.	80
4.9	Summary of ASR for analogues $\text{Ba}_{0.5}\text{Sr}_{0.5}\text{Co}_{0.8-y}\text{Fe}_{0.2+y}\text{O}_{3-\delta}$ ( $0 \leq y \leq 0.8$ )	100

## LIST OF FIGURES

NO		PAGE
1.1	The specific power of energy conversion device as a function of power density at 650 °C (Wachsman & Lee, 2011).	2
1.2	The schematic diagram of SOFCs (Mahato et al., 2015)	3
2.1	Tolerance factors of BSCF at set valence states of Co and Fe metal ions (Shao et al., 2001)	12
2.2	XRD patterns of $Ba_{0.5}Sr_{0.5}Co_{0.8}Fe_{0.2}O_{3-\delta}$ prepare by combined citrate-EDTA method (Lee et al., 2006)	13
2.3	(a) X-ray diffraction patterns of $Ba_{1-x}Sr_xCo_{0.8}Fe_{0.2}O_{3-\delta}$ powder and (b) magnification of (110) peak (Patra et al., 2011)	14
2.4	Lattice parameter of $Ba_{1-x}Sr_xCo_{0.8}Fe_{0.2}O_{3-\delta}$ ( $0.3 \leq x \leq 0.9$ ) as a function of strontium content (Patra et al., 2011)	14
2.5	X-ray diffraction patterns of $Ba_{0.5}Sr_{0.5}Co_{1-y}Fe_yO_{3-\delta}$ oxides with various iron concentrations heated at 1000 °C for 5 hours (Chen et al., 2007).	15
2.6	The magnification of the peak at the Miller index of (110) (Chen et al., 2007).	16
2.7	The lattice constant of a for cubic $Ba_{0.5}Sr_{0.5}Co_{1-y}Fe_yO_{3-\delta}$ as a function of iron content (Chen et al., 2007).	17
2.8	The atomistic modelling of $Ba_{0.5}Sr_{0.5}Co_{0.8}Fe_{0.2}O_{3-\delta}$ (Zhao et al., 2009).	18
2.9	Figure 2.9: Rietveld refinement of the cubic $Ba_{0.5}Sr_{0.5}Co_{0.8}Fe_{0.2}O_{3-\delta}$ using XRD data. (Koster & Mertins, 2003).	19
2.10	Ionic conductivity of fluorite structure oxides (Inaba, 1996).	22
2.11	X-ray diffraction patterns of SDC powders calcined at various temperatures (a) 200 °C; (b) 400 °C; (c) 600 °C; (d) 800 °C (Sha et al., 2006).	24
2.12	XRD patterns of $Ce_{1-x}Sm_xO_{2-x}$ solid solutions synthesis at 1000°C for 3 hours (Huang, 1997).	25
2.13	Lattice parameter of $Ce_{1-x}Sm_xO_{2-x}$ ( $0 \leq x \leq 0.3$ ) (Huang, 1997).	25
2.14	Face centred cubic of fluorite structure (Malavasi et al., 2010).	26



2.15	Complex impedance plane plots for $\text{Ce}_{0.8}\text{Sm}_{0.2}\text{O}_{1.9}$ (a) 238 °C (b) 460 °C (c) 700 °C (d) 901 °C (Zhan et al., 2001).	28
2.16	A schematic representation of the conductivity behaviour of an oxide ionic conductor (Kilner & Waters, 1982).	30
2.17	Arrhenius plots of the $\text{Ce}_{1-x}\text{Sm}_x\text{O}_{1.9}$ ( $0.1 \leq x \leq 0.3$ ) (Anjaneya et al., 2013)	31
2.18	Typical impedance spectrum, as obtained from the two-electrode, symmetric cell at 500°C (Shao, 2004).	33
2.19	Area specific resistance (ASR) of $\text{Ba}_{0.5}\text{Sr}_{0.5}\text{Co}_{1-y}\text{Fe}_y\text{O}_{3-\delta}$ ( $0.2 \leq y \leq 0.6$ ) by using $\text{La}_{0.9}\text{Sr}_{0.1}\text{Ga}_{0.8}\text{Mg}_{0.2}\text{O}_{2.85}$ as electrolyte in air (Pena, et al. 2009).	33
3.1	Flow chart illustrating the steps of synthesis and characterisation of $\text{Ba}_{0.5}\text{Sr}_{0.5}\text{Co}_{0.8-y}\text{Fe}_{0.2+y}\text{O}_{3-\delta}$ ( $0 \leq y \leq 0.8$ ) compound.	37
3.2	Flow chart illustrating of preparation, and characterisation of $\text{Ce}_{0.8}\text{Sm}_{0.2}\text{O}_{1.9}$ .	39
3.3	Flowchart of preparation half-cells BSCF SDC BSCF.	41
3.4	A schematic diagram of sample half-cell BSCF SDC BSCF	41
3.5	(a) The equivalent circuit and (b) complex impedance diagram of two electrolyte and electrode effect denoted as $R_b$ , $R_g$ and $R_e$ represented as bulk, grain boundary and electrode, respectively (Inaba, 1996).	48
3.6	Schematic diagram of impedance jig.	49
4.1	XRD patterns of $\text{Ba}_{0.5}\text{Sr}_{0.5}\text{Co}_{0.8}\text{Fe}_{0.2}\text{O}_{3-\delta}$ heated at 900 °C up to 15 hours.	53
4.2	XRD patterns of $\text{Ba}_{0.5}\text{Sr}_{0.5}\text{Co}_{0.8}\text{Fe}_{0.2}\text{O}_{3-\delta}$ that was heated between 900 and 1100 °C in air.	54
4.3	(a) Lattice parameter and (b) unit cell volume for $\text{Ba}_{0.5}\text{Sr}_{0.5}\text{Co}_{0.8}\text{Fe}_{0.2}\text{O}_{3-\delta}$ as a function of temperature.	55
4.4	Crystallite size of $\text{Ba}_{0.5}\text{Sr}_{0.5}\text{Co}_{0.8}\text{Fe}_{0.2}\text{O}_{3-\delta}$ as a function of temperature.	56
4.5	XRD pattern as a function of $\text{Ba}_{0.5}\text{Sr}_{0.5}\text{Co}_{0.2+y}\text{Fe}_{0.8-y}\text{O}_{3-\delta}$ ( $0 \leq y \leq 0.8$ ) heated at 900 °C for 15 hours.	57
4.6	The enlarge of XRD pattern of $2\theta$ between 30° - 35° of powder synthesized at 900°C in air 15 hours	58

4.7	(a) Lattice parameter and (b) Unit cell volume of $\text{Ba}_{0.5}\text{Sr}_{0.5}\text{Co}_{0.8-y}\text{Fe}_{0.2+y}\text{O}_{3-\delta}$ ( $0 \leq y \leq 0.8$ ) at $900^\circ\text{C}$ for 15 hours as a function cobalt concentration.	60
4.8	(a) SEM micrographs (b) the histogram of particles distribution of $\text{Ba}_{0.5}\text{Sr}_{0.5}\text{Co}_{0.8}\text{Fe}_{0.2}\text{O}_{3-\delta}$ at $1000\times$ .	62
4.9	Rietveld plot of $\text{Ba}_{0.5}\text{Sr}_{0.5}\text{Co}_{0.8}\text{Fe}_{0.2}\text{O}_{3-\delta}$ synthesized at (a) $900^\circ\text{C}$ (b) $950^\circ\text{C}$ (c) $1000^\circ\text{C}$ (d) $1050^\circ\text{C}$ (e) $1100^\circ\text{C}$ in air.	66
4.10	Rietveld plot of $\text{Ba}_{0.5}\text{Sr}_{0.5}\text{Co}_{0.8-y}\text{Fe}_{0.2+y}\text{O}_{3-\delta}$ ( $0.0 \leq y \leq 0.8$ ) (a) $y = 0$ (b) $y = 0.2$ (c) $y = 0.4$ (d) $y = 0.6$ (e) $y = 0.8$ synthesized at $900^\circ\text{C}$ for 15 hours.	69
4.11	XRD patterns of commercial $\text{CeO}_2$ .	71
4.12	XRD patterns of $\text{Ce}_{0.8}\text{Sm}_{0.2}\text{O}_{1.9}$ synthesised at $1450$ and $1500^\circ\text{C}$ in air in the range of 36 hours.	72
4.13	Enlarged XRD patterns of $\text{Ce}_{0.8}\text{Sm}_{0.2}\text{O}_{1.9}$ at $2\theta$ between $28^\circ - 34^\circ$ .	73
4.14	(a) Lattice parameter vs. temperature and (b) Unit cell volume of vs temperature of prepared $\text{Ce}_{0.8}\text{Sm}_{0.2}\text{O}_{1.9}$ heated in air.	74
4.15	Crystallite size vs. temperature for prepared $\text{Ce}_{0.8}\text{Sm}_{0.2}\text{O}_{1.9}$ heated in air.	75
4.16	XRD patterns of pure phase of $\text{Ce}_{0.8}\text{Sm}_{0.2}\text{O}_{1.9}$ (prepared), $\text{Ce}_{0.8}\text{Sm}_{0.2}\text{O}_{1.9}$ (commercial) and $\text{CeO}_2$	76
4.17	Observed (red), calculated (green) and different (purple) profiles from Rietveld refinement of the structure of (a) $\text{CeO}_2$ (b) $\text{Ce}_{0.8}\text{Sm}_{0.2}\text{O}_{1.9}$ (commercial) (c) $\text{Ce}_{0.8}\text{Sm}_{0.2}\text{O}_{1.9}$ (prepared).	81
4.18	Scanning electron micrograph samples of (a) $\text{Ce}_{0.8}\text{Sm}_{0.2}\text{O}_{1.9}$ (prepared) (b) $\text{Ce}_{0.8}\text{Sm}_{0.2}\text{O}_{1.9}$ (commercial) heated at $1350^\circ\text{C}$ for 5 hours.	83
4.19	The conductivity of $\text{CeO}_2$ measured from $450$ to $600^\circ\text{C}$	84
4.20	(a) The complex impedance and (b) the capacitance values of $\text{CeO}_2$ measured at $600^\circ\text{C}$ .	86
4.21	The activation energy of $\text{CeO}_2$ .	87
4.22	Electrical conductivity of $\text{Ce}_{0.8}\text{Sm}_{0.2}\text{O}_{1.9}$ (prepared) that were measured between $250^\circ\text{C}$ and $600^\circ\text{C}$ in air.	88
4.23	(a) The complex impedance and (b) the capacitance value of $\text{Ce}_{0.8}\text{Sm}_{0.2}\text{O}_{1.9}$ (prepared) at $300^\circ\text{C}$ in air.	90
4.24	Complex impedance plots of $\text{Ce}_{0.8}\text{Sm}_{0.2}\text{O}_{1.9}$ (prepared) measured	91

from 300 to 650°C.

4.25	The Arrhenius plot of $\text{Ce}_{0.8}\text{Sm}_{0.2}\text{O}_{1.9}$ (prepared).	92
4.26	Electrical conductivity of $\text{Ce}_{0.8}\text{Sm}_{0.2}\text{O}_{1.9}$ (prepared) and $\text{Ce}_{0.8}\text{Sm}_{0.2}\text{O}_{1.9}$ (commercial) in air at 300 °C.	93
4.27	Complex impedance in of $\text{Ce}_{0.8}\text{Sm}_{0.2}\text{O}_{1.9}$ (prepared) and $\text{Ce}_{0.8}\text{Sm}_{0.2}\text{O}_{1.9}$ (commercial) in air at 300 °C.	94
4.28	The Arrhenius plot of $\text{Ce}_{0.8}\text{Sm}_{0.2}\text{O}_{1.9}$ (prepared) and $\text{Ce}_{0.8}\text{Sm}_{0.2}\text{O}_{1.9}$ (commercial) in air.	95
4.29	The complex impedance of half-cell for composition $\text{Ba}_{0.5}\text{Sr}_{0.5}\text{Co}_{0.8}\text{Fe}_{0.2}\text{O}_{3-\delta}$ measured from (a) 450 °C (b) 500 °C (c) 550 °C (d) 600 °C.	97
4.30	ASR of $\text{Ba}_{0.5}\text{Sr}_{0.5}\text{Co}_{0.8}\text{Fe}_{0.2}\text{O}_{3-\delta}$ from 450°C to 600°C.	98
4.31	The activation energy of half cells BSCF SDC BSCF for analogues $\text{Ba}_{0.5}\text{Sr}_{0.5}\text{Co}_{0.8-y}\text{Fe}_{0.2+y}\text{O}_{3-\delta}$ (a) $y=0$ (b) $y=0.2$ (c) $y=0.4$ (d) $y=0.6$ (e) $y=0.8$	101

## LIST OF ABBREVIATIONS

SOFCs	Solid Oxide Fuel Cells
IT-SOFCs	Intermediate Temperature Solid Oxide Fuel Cells
LSM	Lanthanum Strontium Manganese Oxide
Ni/YSZ	Nickel/Yttria Stabilized Zirconia
TEC	Thermal Expansion Coefficient
LaFeO <sub>3-δ</sub>	Lanthanum Iron Oxide
LaCoO <sub>3-δ</sub>	Lanthanum Cobalt Oxide
YSZ	Yttria Stabilized Zirconia
EDTA	Ethylenediaminetetraacetic acid
XRD	X-ray diffraction
SEM	Scanning Electron Microscopy
SDC	Samarium doped Cerium
BSCF	Barium Strontium Cobalt Iron Oxide
LaGaO <sub>3</sub>	Lanthanum Gallate Oxide
LSGM	Lanthanum Strontium Gallate Magnesium Oxide
CeO <sub>2</sub>	Ceria Oxide
Bi <sub>2</sub> O <sub>3</sub>	Bismuth Oxide
ZrO <sub>2</sub>	Zirconia Oxide
LSC	Lanthanum Strontium Cobalt Oxide
ORR	Oxygen Reduction Reaction
SrCoO <sub>3</sub>	Strontium Cobalt Oxide
La <sub>2</sub> Zr <sub>2</sub> O <sub>7</sub>	Lanthanum Zirconia Oxide
MIEC	Mixed Ionic Electronic Conductor

ASR	Area Specific Resistance
ICDD	The International Centre of Diffraction Data
ICSD	Inorganic Crystal Structure Database
PEM	Polymer Electrolyte Membrane
HT-SOFCs	High Temperature Solid Oxide Fuel Cells

©This item is protected by original copyright

## LIST OF SYMBOLS

$\lambda$	Wavelength
$\sigma$	Conductivity
$\chi^2$	Reduced Chi Square
$2\theta$	Diffraction angle
$Z'$	Real part of Impedance
$-Z''$	Imaginary part of Impedance

©This item is protected by original copyright

## LIST OF EQUATIONS

NO		PAGE
1.1	$2\text{H}_2(\text{g}) + 2\text{O}^{2-} \rightarrow 2\text{H}_2\text{O} + 4\text{e}^-$	3
1.2	$\text{O}_2(\text{g}) + 4\text{e}^- \rightarrow 2\text{O}^{2-}$	3
2.1	$\text{Sm}_2\text{O}_3 + 2\text{Ce}_{\text{Ce}}^{\text{x}} + \text{O}_{\text{O}}^{\text{r}} \rightarrow \text{Sm} + \text{V}_{\text{O}}^{\cdot\cdot} + 2\text{CeO}_2$	23
2.2	$\sigma T = A \exp\left(\frac{-E_a}{kT}\right)$	29
2.3	$V = IR$	31
2.4	$\text{ASR} = \frac{R_p}{2} \times A$	31
3.1	$2d \sin\theta = n\lambda$	42
3.2	$D = \frac{k\lambda}{\beta \cos\theta}$	43
3.3	Gaussian components: $\text{FWHM} = 9(U \tan^2\theta + V \tan\theta + W)^{1/2}$	44
3.4	Lorentzian component: $\text{FWHM} = (X \tan\theta + Y/\cos\theta)^{1/2}$	44
3.5	$R_p = \frac{\sum_i  y_i - y_{ci} }{\sum_i y_i}$	45
3.6	$R_{\text{wp}} = \left[ \frac{\sum_i w_i (y_i - y_{ci})^2}{\sum_i w_i (y_i)^2} \right]^{1/2}$	45
3.7	$\chi^2 = \left[ \frac{R_{\text{wp}}}{R_{\text{exp}}} \right]^2$	46

Struktur dan Sifat Elektrolit dan Elektrod untuk Suhu Pertengahan Sel Oksida Pepejal  
Bahan Api (IT-SOFCs)

**ABSTRAK**

Sel bahan api oksida pepejal (SOFCs) adalah peranti yang digunakan untuk menukarkan dari tenaga kimia kepada tenaga elektrik. Objektif utama tesis ini adalah untuk mengkaji stuktur dan sifat-sifat elektrod dan elektrolit yang digunakan dalam aplikasi suhu pertengahan SOFCs. Komposisi bahan positif elektrod (katod) ialah  $Ba_{0.5}Sr_{0.5}Co_{0.8-y}Fe_{0.2+y}O_{3-\delta}$  ( $0 \geq y \geq 0.8$ ) yang disintesis dengan menggunakan gabungan kaedah EDTA citrate pengkompleks. Fasa tunggal komposisi ini telah diperolehi selepas dipanaskan pada  $900\text{ }^{\circ}\text{C}$  selama 15 jam dengan menggunakan kaedah pengisaran terputus-putus. Belauan sinar x menunjukkan semua sampel membentuk larutan pepejal hingga komposisi terakhir dengan menunjukkan struktur simetri kubus dan kumpulan ruang Pm-3m. Selain itu, struktur hablur stabil sehingga apabila disinter sehingga  $1100\text{ }^{\circ}\text{C}$  di udara. Kemudian, kaedah penyaringan Rietveld dijalankan untuk menegnalpasti perubahan struktur diatas stuktur kubus simetri dengan mengurangkan kandungan kobalt pada  $Ba_{0.5}Sr_{0.5}Co_{0.8-y}Fe_{0.2+y}O_{3-\delta}$ . Hasil dari kajian dengan mengurangkan kandungan kobalt parameter kekisi dan sel unit kekisi telah berkurang. Kation Fe kekal pada kedudukan 1b pada koordinat oktahedral. Selain dari itu, bahan elektrolit dengan komposisi  $Ce_{0.8}Sm_{0.2}O_{1.9}$  telah disintesis menggunakan kaedah konvensional tidak balas pepejal. Komposisi  $Ce_{0.8}Sm_{0.2}O_{1.9}$  yang telah disintesis dibandingkan dengan sampel komesil untuk menentukan struktur hablur, sifat-sifat elektrik dan saiz ira. Hasil dari keputusan tersebut, parameter kekisi dan sel unit kekisi adalah dalam lingkungan yang sama. Walau bagaimanapun, saiz kumin hablur (menggunakan formula Sherrer) dan saiz ira  $Ce_{0.8}Sm_{0.2}O_{1.9}$  untuk komersial sampel lebih kecil berbanding sampel yang disintesis, Kekonduksian elektrik pada suhu  $600^{\circ}\text{C}$  untuk komersial sampel dan sampel yang disintesis masing- masing adalah  $7 \times 10^{-2}$  and  $2 \times 10^{-2} \text{ Scm}^{-1}$ . Walaupun struktur untk sampel yang disediakan dan komersial adalah sama, namun, sifat-sifat electrik untuk sampel komersial adalah lebih tinggi. Daripada prestasi elektrokimia, setengah sel  $Ba_{0.5}Sr_{0.5}Co_{0.4}Fe_{0.6}O_{3-\delta} \mid Ce_{0.8}Sm_{0.2}O_{1.9} \mid Ba_{0.5}Sr_{0.5}Co_{0.4}Fe_{0.6}O_{3-\delta}$  daripada katod komposisi  $Ba_{0.5}Sr_{0.5}Co_{0.4}Fe_{0.6}O_{3-\delta}$  atau  $y = 0.4$  menunjukkan rintangan tertentu kawasan paling rendah (ASR) mengenai  $0.1257 \text{ }\Omega\text{cm}^2$  pada  $600\text{ }^{\circ}\text{C}$  daripada suhu operasi.



## Structure and Properties of Electrolyte and Electrode Materials for Intermediate Temperature Solid Oxide Fuel Cells (IT-SOFCs)

### ABSTRACT

Solid oxide fuel cell (SOFCs) is a device that used to convert from chemical energy to electrical energy. The aim of this thesis is to evaluate the correlation of structure and properties of electrode and electrolyte materials that were used for IT-SOFCs. The positive electrode (cathode) materials with the composition of  $\text{Ba}_{0.5}\text{Sr}_{0.5}\text{Co}_{0.8-y}\text{Fe}_{0.2+y}\text{O}_{3-\delta}$  ( $0 \leq y \leq 0.8$ ) were prepared using combined EDTA citrate complexing method. Phase pure samples were obtained after the samples were heated at  $900^\circ\text{C}$  for 15 hours with intermittence grindings. X-ray diffraction (XRD) showed that all samples were formed full solid solution between both end-members with a cubic symmetry and the space group of Pm-3m. Furthermore, the crystal structure remained stable after heated up to  $1100^\circ\text{C}$  in air. Then, Rietveld refinements were performed to evaluate structural changes on the crystal symmetry by reducing cobalt contents in  $\text{Ba}_{0.5}\text{Sr}_{0.5}\text{Co}_{0.8-y}\text{Fe}_{0.2+y}\text{O}_{3-\delta}$ . Results indicated that reducing Co contents decreased the lattice parameters and unit cell volume. Fe cation was remained at the 1b-site with the octahedral coordination. On the other hand, electrolyte material with the composition of  $\text{Ce}_{0.8}\text{Sm}_{0.2}\text{O}_{1.9}$  was prepared using conventional solid-state synthesis route. The prepared  $\text{Ce}_{0.8}\text{Sm}_{0.2}\text{O}_{1.9}$  was compared with the commercial sample to determine their structure, electrical properties, and grain size. Results show that the lattice parameters and unit cell volume of the prepared and commercial  $\text{Ce}_{0.8}\text{Sm}_{0.2}\text{O}_{1.9}$  were similar within errors. But crystallite size (using Scherrer's formula) and grain size (SEM micrograph) of the commercial  $\text{Ce}_{0.8}\text{Sm}_{0.2}\text{O}_{1.9}$  were relatively smaller than the prepared sample. Furthermore, the measured electrical conductivities of commercial and prepared  $\text{Ce}_{0.8}\text{Sm}_{0.2}\text{O}_{1.9}$  were  $7 \times 10^{-2}$  and  $2 \times 10^{-2} \text{ Scm}^{-1}$  at  $600^\circ\text{C}$ , respectively. The structure of commercial and prepared  $\text{Ce}_{0.8}\text{Sm}_{0.2}\text{O}_{1.9}$  are similar, however, electrical properties of commercial  $\text{Ce}_{0.8}\text{Sm}_{0.2}\text{O}_{1.9}$  is relatively much better than prepared  $\text{Ce}_{0.8}\text{Sm}_{0.2}\text{O}_{1.9}$ . On the other hand, the electrochemical performance of in-house prepared half-cell  $\text{Ba}_{0.5}\text{Sr}_{0.5}\text{Co}_{0.4}\text{Fe}_{0.6}\text{O}_{3-\delta} | \text{Ce}_{0.8}\text{Sm}_{0.2}\text{O}_{1.9} | \text{Ba}_{0.5}\text{Sr}_{0.5}\text{Co}_{0.4}\text{Fe}_{0.6}\text{O}_{3-\delta}$  shows the lowest Area Specific Resistance (ASR) about  $0.1257 \Omega\text{cm}^2$  at  $600^\circ\text{C}$ .

# CHAPTER 1

## INTRODUCTION

### 1.1 Solid Oxide Fuel Cells (SOFCs)

There is an increasing electrical energy demand over the world to power all electrical devices. The major demand mainly used for construction, stationary power sources and transportations sector (Abas et al., 2015). Fossil fuel from natural resources is a main resource used to generate electricity. However, fossil fuel is non-renewable and not sustainable energy resources. Therefore, alternative energy resources have been intensively investigated to replace the usage of natural resources.

Solid oxide fuel cell (SOFCs) is one of the alternatives of clean and sustainable energy resources to generate electricity. SOFCs is used to generate electricity from chemical reaction between hydrogen ( $H_2$ ) and oxygen ( $O_2$ ) gas (Dupuis, 2011). SOFC offers high efficiency energy conversion (about 60 to 80%) and very low environmental impact to ensure future clean energy generation (Shao et al., 2012). Furthermore, SOFC is exhibited the highest specific power (in  $W.kg^{-1}$ ) and power density (in  $W.cm^{-3}$ ) at operating temperature of  $650^\circ C$  compared to other alternative energy conversion devices such as combustion engines, PEM fuel cells, photovoltaic cells, electromagnetic generator and thermoelectric generator as shown in Figure 1.1. Thus, SOFC is

considered as the most promising electrical power generation device for sustainable energy resource.

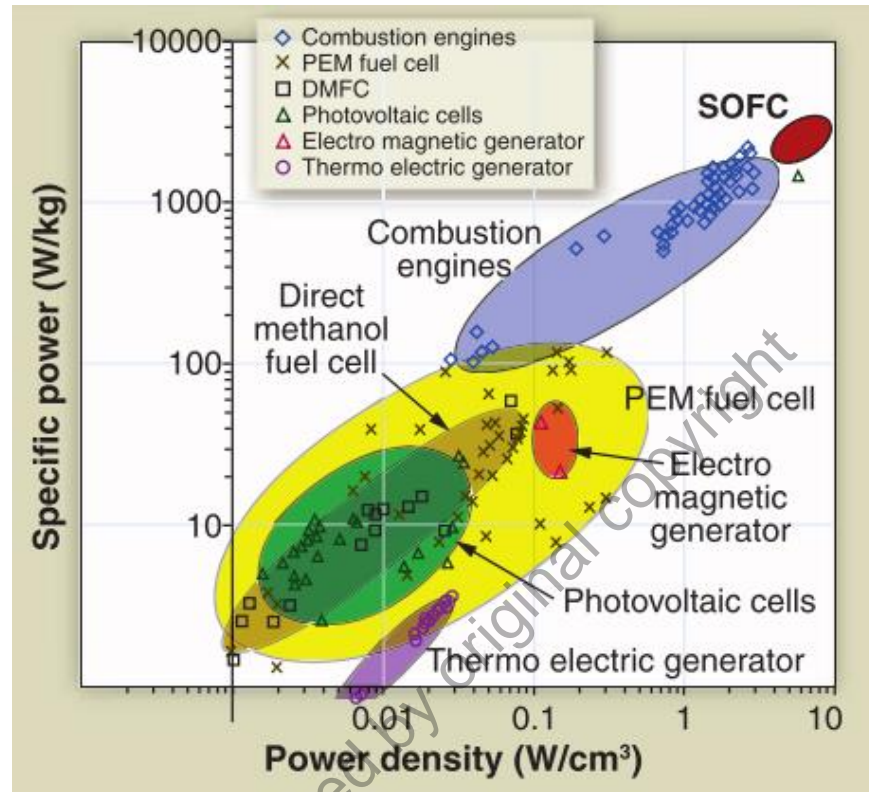


Figure 1.1: The specific power of energy conversion device as a function of power density at 650°C (Wachsman & Lee, 2011).

A SOFCs consist of two porous electrodes; anode (as negative electrode), cathode (as positive electrode) and separated by highly dense solid electrolyte. During the chemical conversion process, hydrocarbon was used as a fuel to supply  $H_2$  gas to anode while air was used to supply  $O_2$  gas to cathode. At the anode, oxidation process occurs and  $H_2$  was converted to  $H^+$  ions and released electrons. The electrons were flowed to the external circuit and move to cathode. The reduction process was occurred when  $O_2$  from air reacted with the flux of electrons at the cathode to produce  $O^{2-}$  ions. Then, the  $O^{2-}$  ions were diffused through electrolyte toward the anode. In the mean time,  $O^{2-}$  ions at the anode were reacted with  $H^+$  ions to produce  $H_2O$  as a by-product. Therefore, continuous oxidation and reduction processes at the both anode and cathode,

respectively, resulting electricity was generated (Mahato et al., 2015). Figure 1.2 shows a schematic diagram of SOFCs. The electrochemical reaction occurred at the anode and cathode as shown in equation (1.1) and (1.2), respectively.

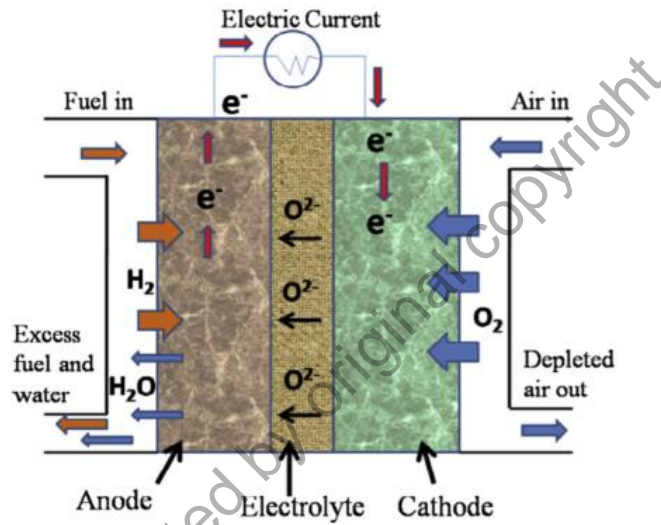


Figure 1.2: The schematic diagram of SOFCs (Mahato et al., 2015).

Conventional SOFCs are operated at high temperature between 800 and 1000°C. The high operating temperature is necessary for conventional SOFCs to improve kinetic reactions of the electrode and to reduce ohmic drop at the electrolyte (Zhou et al., 2009). However, several problems occurred at the high operation temperature such as interface-reactions problem between electrode and electrolyte, materials compatibility, possibility of crack formation of cells due to thermal expansion coefficient (TEC) mismatch and high cost (Ahmadrezaei et al., 2013). Thus, these problems had led to the development of the new type of SOFCs that able to operate at relatively lower temperature (between 500 and 700°C) compared to conventional SOFCs (HT-SOFCs) known as the Intermediate Temperature Solid Oxide Fuel Cells (IT-SOFCs).

IT-SOFCs are offers several advantages such as the reduction of energy consumptions, lowering the operation and setup cost, improved materials compatibility of components, enhancing the durability and reliability at long-term operation, and more widely selection of materials could be used (Huang et al, 2012):

## **1.2 Properties of SOFCs components**

### **1.2.1 Electrolyte**

Electrolyte is a medium for diffusion of oxygen ions from cathode as a positive electrode to anode as a negative electrode. Electrolyte should only allow oxygen ions diffuse from cathode to anode but electrically resistive. Therefore, electrolyte materials must exhibit excellent ionic conductivity, chemical resistant, and high thermal stability at the operating temperature. Yttria stabilized zirconia (YSZ) is an example of conventional electrolyte used for SOFC. YSZ has high ionic conductivity, excellent chemical resistivity and thermal stability at an operation temperature of about 1000°C. There are seven general criteria of solid electrolyte could be used in SOFCs, such as the following (Mahato et al. 2015):

1. Easy to fabricate and have small thickness,  $L$  and large area,  $A$ .
2. Has ionic conductivity in range of  $10^{-3}$  to  $10^{-1} \text{Scm}^{-1}$  at operating temperature.
3. Have chemical stability or inert in oxidizing or reducing atmosphere.
4. Low cost of materials and fabrication.
5. Long-term stability at operating temperature.
6. Match TEC with electrode and interconnector.
7. High long-term reliability (high strength and high durability).

### 1.2.2 Anode

Anode is a negative electrode in SOFCs. A porous anode should be electrically conductive to facilitate oxidation process for conversion of H<sub>2</sub> from fuel to H<sup>+</sup> ions and electrons. Thus, enables electrons to flow from the reaction site to the current collector. Thus, a conventional anode of SOFCs is made up by cermet which is the combination of ceramic and metallic materials. Ni/YSZ is a common anode materials used in SOFCs. The criteria of an anode are (Taroco, et al. 2009):

1. High mixed ionic and electronic conductivity about 1000 Scm<sup>-1</sup>.
2. TEC values are matches those of the adjoining components (electrolyte).
3. High chemical stability under a reducing atmosphere.
4. Large triple phase boundary.
5. High electrochemical or catalytic activity for the oxidation of the selected fuel gas.
6. High porosity (20 - 40 %) adequate for the fuel supply.

### 1.2.3 Cathode

Cathode is a positive electrode in SOFCs. A porous cathode should be electrically conductive to facilitate a flux of electrons from anode through external circuit to react with oxygen gas. Therefore, reduction process of O<sub>2</sub> to O<sup>-2</sup> ions could be accelerated. Lanthanum strontium manganese oxide (LSM) is an example of conventional cathode material that was used at high temperature operations of SOFCs. Generally, the requirement for SOFCs cathode are listed as follows (Sun et al., 2009):

1. High electronic conductivity (approximately above 100 Scm<sup>-1</sup> under oxidizing atmosphere).

2. Should have adequate porosity (approximately 30 to 40%) to diffuse gaseous oxygen.
3. Thermal expansion coefficient (TEC) similar between an electrolyte and interconnector.
4. Stable in oxidizing environment.
5. Large triple phase boundary for electrochemical reaction of electron, oxygen ions and gas.
6. Easily fabricated and relatively low cost.

### 1.3 Problems Statement

High temperature SOFCs (HT-SOFCs) that is operated at about 800 to 1000°C introduces a several drawbacks to cell components and also limited of trials selection. Thus, IT-SOFCs was developed to ensure the promising future clean of power generation. IT-SOFC offers very low carbon emissions, highly efficient (~80 %) and excellent fuel flexibility compared to the HT-SOFCs. Furthermore, IT-SOFCs also has a variety of advantages such as shortens time taken for start-up/shutdown, extended operation lifetime and minimizes thermal and sealing degradations (Zhao et al., 2009).

The composition of  $\text{Ba}_{0.5}\text{Sr}_{0.5}\text{Co}_{0.8}\text{Fe}_{0.2}\text{O}_{3-\delta}$  was reported as excellent cathode materials for IT-SOFCs compared to  $\text{La}_{0.2}\text{Sr}_{0.8}\text{Co}_{0.8}\text{Fe}_{0.2}\text{O}_{3-\delta}$  (Ahmadrezaei et al., 2013). However, higher amount of cobalt content in  $\text{Ba}_{0.5}\text{Sr}_{0.5}\text{Co}_{0.8}\text{Fe}_{0.2}\text{O}_{3-\delta}$  had raised to an environmental issue, high cost, structural instability and high thermal expansion coefficient (Chen et al., 2007). Thus, different concentrations of cobalt contents in  $\text{Ba}_{0.5}\text{Sr}_{0.5}\text{Co}_{0.8}\text{Fe}_{0.2}\text{O}_{3-\delta}$  were investigated in this project.

On the other hand,  $\text{Ce}_{0.2}\text{Sm}_{0.8}\text{O}_{1.9}$  was reported as the best candidate for electrolyte materials to be used in IT-SOFCs. However, preparation of  $\text{Ce}_{0.2}\text{Sm}_{0.8}\text{O}_{1.9}$  commonly involved complex wet methods such as sol-gel and combustion methods (Hui et al., 2007). Thus, we attempted to simplify the synthesis method by using conventional solid-state synthesis route. After that, a comparison between commercial and in-house prepared SDC was performed to evaluate their properties. Then, electrochemical performance of half-cell between  $\text{Ba}_{0.5}\text{Sr}_{0.5}\text{Co}_{0.8}\text{Fe}_{0.2}\text{O}_{3-\delta}$  |  $\text{Ce}_{0.2}\text{Sm}_{0.8}\text{O}_{1.9}$  |  $\text{Ba}_{0.5}\text{Sr}_{0.5}\text{Co}_{0.8}\text{Fe}_{0.2}\text{O}_{3-\delta}$  were evaluated.

#### 1.4 Objectives

The objectives of this study are:

- i. To synthesise and characterise electrolyte and positive electrode (cathode) materials for IT-SOFCs component.
- ii. To determine crystallographic properties of  $\text{Ce}_{0.8}\text{Sm}_{0.2}\text{O}_{1.9}$  as an electrolyte and  $\text{Ba}_{0.5}\text{Sr}_{0.5}\text{Co}_{0.8-y}\text{Fe}_{0.2+y}\text{O}_{3-\delta}$  ( $0 \leq y \leq 0.8$ ) as a cathode.
- iii. To evaluate the electrical and electrochemical properties of electrolyte ( $\text{Ce}_{0.8}\text{Sm}_{0.2}\text{O}_{1.9}$ ) and half cells of BSCF|SDC|BSCF, respectively.